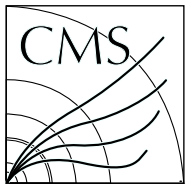

The Compact Muon Solenoid Experiment

CMS Note

Mailing address: CMS CERN, CH-1211 GENEVA 23, Switzerland

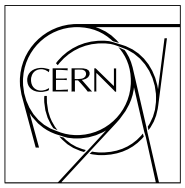

July 4, 1997

DETECTION OF PHOTONS GENERATED IN $PbWO_4$ SCINTILLATOR CRYSTALS

S. Baccaro[a], B. Borgia[b], F. Cavallari[b], I. Dafinei[b], M. Diemoz[b], A. Festinesi[a], E. Longo[b], M. Montecchi[a], G. Organtini[c], A. Piegari[a]

INFN, Sezione di Roma, Roma, Italy

[a] *ENEA-INN/TEC, Casaccia Research Centre, Roma,Italy*

[b] *Department of Physics, Università "La Sapienza", Roma, Italy*

[c] *Department of Physics, Università "Roma TRE", Roma, Italy*

Abstract

This work deals with the optical characterisation of the surface of EG&G and Hamamatsu APD's and performance of an antireflection coating made of Y_2O_3 and deposited on a PWO test piece. The effectiveness of antireflection treatments of PWO and Si surfaces is evaluated in a simplified and a realistic situation by means of the ratio of "detected to emitted photons". The complex refractive index of the Dow Corning 02-3067 optical grease is also reported.

1 Introduction

Lead tungstate $PbWO_4$ (PWO) is chosen as scintillating medium for the electromagnetic calorimeter of the CMS experiment at LHC (CERN) [1]. PWO is a negative uniaxial crystal with refractive indexes close to 2.3 [2] and two main emission bands located at 420nm (blue) and at 520nm (green) [3]. For the CMS purpose, crystals are cut as pyramid frustum (section about $2x2cm^2$, length 23.5cm) and the photons generated inside the PWO scintillator are detected by an avalanche photodiode (APD) facing the major base of the crystal. Between PWO and APD is interposed a coupling medium (CM) (air, optical grease or glue) having a refractive index lower than the PWO one, therefore total reflection occurs when the incidence angle of the photon on the PWO//CM interface is greater than the critical angle. The rate of detected photons is further reduced by the reflections at the PWO//CM and CM//APD interfaces. The critical angle can be maximised by adopting a CM with a refractive index as close as possible to the PWO one; the reflections can be reduced covering both PWO and Si surface with antireflection coatings.

The present paper reports on the optical characterisation of the surface of EG&G and Hamamatsu APD's and performance of an antireflection coating made of Y_2O_3 and deposited on a PWO test piece. The effect of antireflection treatments of PWO and Si surfaces in the optical coupling between PWO and APD is evaluated in a simplified and a realistic situation.

In order to make easier the reading, the meaning of the symbols used in the paper are summarised in Table 1.

Table1: symbols used through the paper

Symbol	Meaning
PWO	$PbWO_4$
APD	avalanche photodiode
W	transparent window covering the Si surface of the APD; when W is referred to computed quantities, the material composing W is reported in brackets
CM	coupling medium; it is placed between PWO and APD
TG	transparent glue; it is placed between W and Si surfaces in EG&G APD's
DG	Dow Corning 02-3067 optical grease
A//B	plane interface between the semi infinite media A and B
A//B//C	the medium B is enclosed between the semi infinite media A and C; the A//B and B//C interfaces are plane and parallel to each other
AR	antireflection coating; it is deposited on the surface of A or B in order to reduce the reflectance of the A//B interface (A//AR//B)
λ	wavelength
n	refractive index
k	extinction coefficient; k is related to the absorption coefficient ($\alpha=4\pi k/\lambda$) and the absorption length (α^{-1})
d	thickness
D/E	ratio of photons detected by the APD to photons emitted inside the PWO

2 APD surface characterisation

The APD is substantially composed of a silicon (Si) wafer properly doped along planes parallel to the surface. In the visible light spectrum, the considerable reflectance of the air//Si interface (about 40%) requires the adoption of an antireflection coating (AR), consisting of a suitable quarter wave thick dielectric layer [4], in order to enhance the ratio of the detected photons. Silicon dioxide (SiO_2) AR reduces the reflectance to about 15% and it is the most commonly used material because of its low price. On the other hand, SiO_2 is damaged by neutrons and gamma rays copiously produced in the CMS experimental environment. Recently EG&G and Hamamatsu produce APD coated with silicon nitride (Si_3N_4) which has a better radiation resistance.

The characteristic of the examined APD's are shown in Table 2. The EG&G APD belong to the batch received in spring '96. The Hamamatsu APD's belong to the "batch B", received from the producer in summer '96.

Table 2: the examined APD's

#	Producer	coating	Irradiation
397A	EG&G	Si_3N_4	before and after $4\ 10^{13}$ neutron/cm^2
BA-5	Hamamatsu	SiO_2	$4\ 10^{13}$ neutron/cm^2
BB-5	Hamamatsu	SiO_2	$4\ 10^{13}$ neutron/cm^2
BC-5	Hamamatsu	SiO_2	$4\ 10^{13}$ neutron/cm^2
BC-17	Hamamatsu	SiO_2	not irr.
BC-25	Hamamatsu	SiO_2	$4.9\ 10^{11}$ neutron/cm^2
BE-5	Hamamatsu	SiO_2	$4\ 10^{13}$ neutron/cm^2
BA-1N	Hamamatsu	Si_3N_4	not irr.

At the present time APD's are enclosed in a capsule and covered with a transparent window (W). In the EG&G APD prototype the window is sealed to the capsule with some transparent glue (Fig. 1a). Hamamatsu adopts a rubber window which completely fills the capsule-room and covers the Si surface together with the electric contacts (Fig.1b). The window thickness (d) is evaluated by means of an optical microscope (Fig. 2). Let n be the refractive index of the window and h the difference between the heights of the microscope plate for which, respectively, the window external surface and its image, reflected by the Si surface, are focused. The optical path nh is equal to $2d$, therefore

$$d = nh/2 \tag{1}$$

As reported later, the refractive index of EG&G and Hamamatsu APD windows results to be equal to glass (n~1.53) and fused silica (n~1.46) one respectively. In the case of the EG&G APD the front window surface is plane and parallel to the Si surface and d = 0.73 ± 0.01 mm. The surface of the rubber window of the

Hamamatsu APD's is concave with a focus length of about 5cm; in the centre of the active area the thickness averaged over seven different APD (see Table 2) is 0.27 mm, the minimum is 0.19 mm and the maximum 0.37 mm. Along the border of the active area d is typically 15% greater than the central value. In any case the window thickness is much larger than wavelengths of the visible range, so there is not optical interference between the window surfaces.

Once tests and optical measurements on the EG&G APD were accomplished, we removed the window and found a layer of transparent glue (TG) between window and Si surfaces. The thicknesses of window and glue layer, respectively measured with a calliper and by the above mentioned optical microscope method, are 0.70 ± 0.05 mm and 0.030 ± 0.01 mm. Fig. 3 compares the refractive index of the window, deduced from transmittance and reflectance measured at normal incidence with a commercial spectrophotometer, with the refractive index of the SiO_2 (fused silica) [5] which, as discussed in the following, will be assigned to the EG&G transparent glue (TG). In the same wavelength range, the extinction coefficient of the glass window is $k < 1\ 10^{-6}$.

The measurement of reflectance at normal incidence, performed equipping the spectrophotometer with an integrating sphere, gives information about the coating of the Si surface. Fig. 4 shows the experimental reflectance of the "397A" EG&G APD. The minimum at 530 nm is due to the Si_3N_4 coating. The same figure also shows the reflectance of the system air//W(glass)//TG(SiO_2, k=0)// Si_3N_4(59nm)//Si computed using the complex refractive indexes of Si and Si_3N_4 found in literature [5], and shown in Fig. 5a, and where the refractive index of the transparent glue layer (TG) is the same of the SiO_2 (k=0). The computed reflectance is in a good agreement with the experimental curve excepted at shorter wavelengths where the experimental reflectance is lower than the computed one as if some absorption occurs. The agreement is considerably improved when the extinction coefficient shown in Fig. 5b is assigned to the 30 μm thick glue layer (TG). Fig. 4 also shows Si_3N_4 antireflection coating is more effective in the 400-520 nm range when the coating thickness is about 50 nm. The APD reflectance does not change after the irradiation, performed at the TAPIRO plant of ENEA-Casaccia, with $4\ 10^{13}$ neutrons/cm^2 that is above the dose expected for 10 years of CMS running [6].

Six of the seven examined Hamamatsu APD are coated with SiO_2 and some of them were irradiated by various doses of neutrons up to the maximum dose of $4\ 10^{13}$ neutrons/cm^2 (see Table 2). As shown in Fig. 6, the reflectance is not significantly affected by such an irradiation and it is well reproduced with the model "air//W(SiO_2)//Si" where the refractive index of the rubber window (W) is the same of the SiO_2 coating with k=0. As a consequence, the SiO_2 coating is not distinguishable from the rubber window which is in direct optical contact with the SiO_2 coated Si surface and no interference appears in the reflectance spectrum. The slight disagreement with the experimental curve occurring at longer wavelengths is probably due to a weak absorption of the rubber window, considered perfectly transparent in the model.

The measured reflectance of the Si_3N_4 coated "BA-1N" Hamamatsu APD is reported in Fig. 7 together with the computed curve based on the model "air//W(SiO_2)// Si_3N_4(41nm)//Si"; the agreement is satisfactory. Again, as the figure shows, the effect of the Si_3N_4 antireflection coating would be more effective in the 400-520 nm range with a coating thickness of about 50 nm. In the following we will always consider this optimal thickness.

In the end we consider the material used for antireflection coating of the Si surface. Silicon nitride (n~2.0) is a good choice when the Si surface is interfaced with air. In the actual case the Si surface of EG&G and Hamamatsu APD's is coupled with a medium having the refractive index of the fused silica, therefore a coating with a higher refractive index, like titanium dioxide (TiO_2, n~2.5), would further improve the transmission of the system W(SiO_2)//AR//Si by about 5% as reported in Fig. 8a (versus the wavelength) and Fig. 8b (versus the incidence angle). Obviously the radiation resistance of this material should be verified. In any case, it must be noticed the reduction due to a AR of the transmittance dependency on the polarisation.

3 Antireflection coating for the PWO//CM interface

Among the photons generated inside the PWO scintillator, only those impinging the major base surface with an angle θ lower than the critical angle are able to cross the interface PWO//CM. As a matter of fact, the available CM's have a refractive index n_{CM} lower than the PWO one (n_{PWO} ~ 2.3) therefore the total reflection occurs when θ is greater than the critical angle equal to

$$\theta_C = arcsin(n_{CM}/n_{PWO}) \quad (3)$$

For an isotropic source located inside PWO, close to PWO//CM, the ratio of emerging to emitted photons is

$$2\pi(1-cos\ \theta_C)/4\pi \quad (4)$$

This ratio is 0.0497 and 0.121 respectively for air (θ_C ~ 26 deg) and for optical grease (θ_C ~ 41 deg). The use of CM with the highest refractive index is clearly the most convenient. In the following we consider the CM composed by DOW Corning 02-3067 optical grease (DG) whose refractive index and absorption length, computed from transmittance and reflectance measured at normal incidence, are reported in Fig. 9. For wavelengths greater than 400nm the grease refractive index is very similar to the SiO_2 (fused silica) one. In the wavelength range of PWO scintillation light the absorption due to an optical grease layer, 0.1 mm thick, is less than 0.3%.

The rate of the emerging photons, that is photons having an incident angle lower than θ_C, is further reduced by reflection at the PWO//DG interface. This reflection can be reduced by coating the major base surface of the PWO crystal with a quarter wave thick film with refractive index equal to $\sqrt{n_{PWO}n_{DG}}$. This optimal value is reported in Fig. 10 both for the ordinary and the extraordinary PWO refractive index. Yttrium Oxide (Y_2O_3) has a refractive index [7] close enough to the optimal value, as shown in the same figure ("Y_2O_3 bulk"). Two quarter wave thick Y_2O_3 films were deposited on the surfaces of a PWO test piece (1.9mm thick) in order to verify the feasibility of the deposition, the actual refractive index of the film and the resistance to neutron irradiation. The deposition of the Y_2O_3 films, performed with a Balzer electron beam evaporator BAK 640 equipped with an ion gun (Ion Tech), was ion assisted with 20 $\mu A/cm^2$ of 150 eV Xe^+ ions [8]. The deposition rate was 0.2 nm/sec. The PWO substrate was heated at 200 °C and the oxygen partial pressure was 3.5 10^{-4} torr in the deposition chamber.

Fig. 11 shows transmittance and reflectance, measured at normal incidence with unpolarised light, of uncoated and coated PWO test pieces. The experimental curves are well reproduced by assuming that the films are perfectly transparent (k=0), 62.5 nm thick and with the refractive index of a material composed by 76% in

volume of Y_2O_3 and 24% of air, computed according to the effective medium approximation [9]. The refractive index of the deposited film, although lower than those reported in literature, is close enough to the optimal one, and is shown in Fig.10 ("Y_2O_3 film").

The transmittance of the interfaces PWO//DG and PWO//Y_2O_3(62.5nm)//DG is simulated at normal incidence versus the wavelength (Fig.12) and at 420 nm and 520nm versus the incidence angle (Fig. 13a and Fig. 13b). From these figures some observations follow: i) the antireflection coating does not affect the critical angle; ii) a quarter wave thick Y_2O_3 film works as a good antireflection coating in the whole PWO scintillation light wavelength range even if the refractive index is 7% lower than the optimal value; iii) the antireflection coating reduces the transmittance dependence on the light polarisation.

The coated PWO test piece was irradiated with neutrons with a dose of 2 10^{12} neutrons/cm^2 and, successively, 2 10^{13} neutrons/cm^2, equivalent to the dose for 10 years of CMS running [6]. No variation was found in the transmittance and reflectance spectra.

In conclusion, Y_2O_3 is easy to deposit on PWO, resistant to neutron irradiation and able to reduce the reflectance at the PWO//DG interface in the whole PWO scintillation light range.

4 Optical coupling between PWO and APD

Once the PWO major base and the APD front surfaces are characterised, the transmittance throughout the system PWO//(AR)//DG//W//(TG)//(AR)//Si can be computed for every incidence angle, for *p* and *s* polarisations, on the basis of the complex refractive indexes and the thicknesses of the involved materials. More precisely, the simulation implies the subdivision of the system in several simpler sub-systems belonging to one of the following canonical cases whose relationships are reported in literature:

i) two semi-infinite media separated by a thin film [4];

ii) two semi-infinite media separated by a third medium having a thickness much greater than the light wavelength so that there is not interference between the two boundaries [10].

These sub-systems are then considered like simple boundaries and assembled again one to each other in a new canonical system i) or ii). It should be emphasised that *s* and *p* polarisations must be treated separately up to the end of the whole procedure and they can be averaged only *a posteriori*.

The following optical coupling (OC) are considered

OC1: EG&G APD where the 30 μm thick glue layer (TG) with the same refractive index of SiO_2 is considered absorbing according to the characterisation discussed in Section 2 (PWO//DG//W(glass)//TG(SiO_2;k>0)//Si_3N_4(50nm)//Si);

OC2: Hamamatsu APD, SiO_2 AR coated, where the APD window (W) can not be distinguished from the SiO_2 AR film because they have the same refractive index (PWO//DG//W(SiO_2)//SiO_2//Si);

OC3: Hamamatsu APD, Si_3N_4 coated (PWO//DG//W(SiO_2)//Si_3N_4(50nm)//Si);

OC4: as OC3 but with a TiO_2 AR coating on the APD (PWO//DG//W(SiO_2)//TiO_2(45nm)//Si);

OC5: as OC4 but with a Y_2O_3 AR coating on the PWO major base surface (PWO//Y_2O_3(62.5nm)//DG//W(SiO_2)//TiO_2(45nm)//Si).

For all cases, the transmittance from PWO to Si is computed versus the wavelength at normal incidence (Fig. 14a), versus the incidence angle at 420nm (p-polarised Fig. 14b, s-polarised Fig.14c) and 520nm (p-polarised Fig. 14d, s-polarised Fig.14e). In all cases DG is Dow Corning 02-3067 optical grease and the AR thickness optimises the transmission in the scintillation wavelength range. Once again from these figures follow that: i) the antireflection coating does not affect the critical angle; ii) a quarter wave film works as a good antireflection coating in the whole PWO scintillation light wavelength range; iii) the antireflection coating reduces the transmittance dependence on the light polarisation.

The performances of the above mentioned optical couplings are evaluated by means of the ratio "detected to emitted photons" (D/E) reported in Table 3 and computed for the two cases:

S) simplified case: isotropic source placed in a PWO parallelepiped with semi infinite length and infinite absorption length, coupled to an APD with active area greater than the PWO base surface;

R) realistic case: isotropic sources randomly placed according to the electromagnetic shower distribution due to a 50 GeV electron. The electron hits the centre of the minor base of a pyramid frustum shaped PWO crystal (1.8x1.8cm^2 minor base, 2.1x2.1cm^2 major base, 23cm length, according to the '95 geometry) with 1 meter absorption length and coupled with a realistic APD. The active areas of the EG&G and Hamamatsu APD's are respectively square (A = 5x5mm^2 = 25.0mm^2) and circular (∅=5mm, A=19.6mm^2).

The ratio D/E was computed by the equation

$$D/E = \frac{2\pi \int_0^{\pi/2} T(\vartheta) \sin\vartheta d\theta}{4\pi} \qquad (5)$$

for the simplified (S) case and by a proper Montecarlo simulation for the realistic (R) case.

Table 3: D/E and improvement with respect to OC2.

	D/E (%) and (OCJ/OC2) at λ = 420 nm		D/E (%) and(OCJ/OC2) at λ = 520 nm		<OCJ/OC2>	
	S	**R**	**S**	**R**	**S**	**R**
OC1	8.56 (1.20)	1.44 (1.50)	9.40 (1.13)	1.95 (1.38)	1.16	1.44
OC2	7.11 (1.00)	0.96 (1.00)	8.29 (1.00)	1.41 (1.00)	1.00	1.00
OC3	9.11 (1.28)	1.22 (1.27)	9.71 (1.17)	1.60 (1.13)	1.22	1.20
OC4	9.79 (1.38)	1.31 (1.36)	10.13 (1.22)	1.64 (1.16)	1.30	1.26
OC5	10.42 (1.47)	1.40 (1.46)	10.53 (1.27)	1.71 (1.21)	1.37	1.33

In both the cases PWO is considered optically isotropic, PWO surfaces are polished, there is not photon scattering inside PWO and on the surfaces, there is not wrapping and the transmittance is averaged on the *p* and *s* polarisations.

We point out some differences between S and R case. In the R case, the APD active area is 5.7% and 4.4% of the PWO major base surface, respectively for EG&G and Hamamatsu prototype, and some photons are absorbed inside the PWO. On the other hand the ratio D/E is increased by the focusing effect due to the tapered shape and by the reflection at the surface 1.8x1.8cm^2. According to Table 3, the detected photons in R are about 15% respect to S for all the examined optical couplings.

With respect to the Si_3N_4 coated Hamamatsu APD (OC3), in the S case the performance of the EG&G APD (OC1) is slightly impaired by the absorption of the transparent glue layer (TG) placed between the window and the Si_3N_4 coated Si surfaces. In the R case, due to the larger active area, the EG&G APD exhibits the highest D/E ratio. The performance of the SiO_2 coated Hamamatsu APD (OC2) is surpassed by a Si_3N_4 (OC3) or by a TiO_2 (OC4) AR coating on the Si, respectively, by about 21% or 28% (averaging the S and R values). According to the simulation, we expect a further improvement of 7% with the Y_2O_3 AR coating on the PWO major base surface.

5 Conclusions

The detection of photons generated inside the PWO by the APD facing the major base of the pyramid frustum shaped crystal is reduced by two main factors: the total reflection and the reflections at the crossed boundaries.

The total reflection imposes a cut-off value, the critical angle, to the photons impinging on the major base. This critical angle depends on the ratio of the lowest refractive index of the crossed media, and the PWO one. Actually such a material is the transparent glue (TG) and the rubber window ($W(SiO_2)$) respectively for EG&G and Hamamatsu APD's prototypes and both have the refractive index of SiO_2 (fused silica) thus $\theta_C \sim 41$ deg. The adoption of a CM with $n_{CM} > 1.5$ can bring benefit if the refractive index of these components is also enhanced.

The main reflections at the boundaries of the crossed media, are those at the W//Si and PWO//CM interfaces. Both can be reduced in the whole PWO scintillation wavelength range by means of a quarter wave thick dielectric layer. As very noticeable properties this antireflection coating does not affect the critical angle and reduces the transmittance dependence on the light polarisation. The APD window has the refractive index close to the fused silica, therefore a SiO_2 coating on the Si surface has no effect. The ratio "detected to emitted photons" (D/E) is improved by 22% with a Si_3N_4 ($n \sim 2$) AR coating. Using a material with an higher refractive index, like titanium dioxide (TiO_2, $n \sim 2.5$), the improvement is 29%. The resistance to neutron and gamma irradiation of this material should be verified. Yttrium oxide was investigated as a possible material for the AR coating of the PWO major base surface. Y_2O_3 is easy to deposit on PWO, resistant to neutron irradiation and, according to the reported simulations, it is expected to be able to further enhance D/E by 7%.

References

[1] "The Compact Muon Solenoid Technical Proposal", CERN/LHCC 94-38.

[2] S. Baccaro, L. M. Barone, B. Borgia, F. Castelli, F. Cavallari, I. Dafinei, F. de Notaristefani, M. Diemoz, A. Festinesi, E. Leonardi, E. Longo, M. Montecchi, G. Organtini, "Ordinary and extraordinary complex refractive index of the Lead Tungstate ($PbWO_4$) crystal", Nucl. Inst. and Meth. **A 385** (1997) 209-214.

[3] J. A. Groening, G. Blasse, "Some new observations on the luminescence of $PbMoO_4$ and $PbWO_4$", J. Solid State Chem. **32** (1980) 9-20.

[4] H. A. Macleod, "Thin Film Optical Filters", Cap.2, 2nd edition, Macmillan, New York, 1986.

[5] E. D. Palik, "Handbook of Optical Constants of Solids", Academic Press, London, 1985.

[6] M. Huhtinen, "Radiation environment simulations for the CMS detector", CMS TN 95-198.

[7] E. D. Palik, "Handbook of Optical Constants of Solids II", Academic Press, London, 1991.

[8] T. Itoh, "Ion Beam Assisted Film Growth", Elsevier, Amsterdam, 1989.

[9] See, for example, Cap. 5 of [7].

[10] L. Vriens and W. Rippens, "Optical constants of absorbing thin solid films on a substrate", Appl. Opt. **22** (1983) 4105-4110.

a) EG&G APD

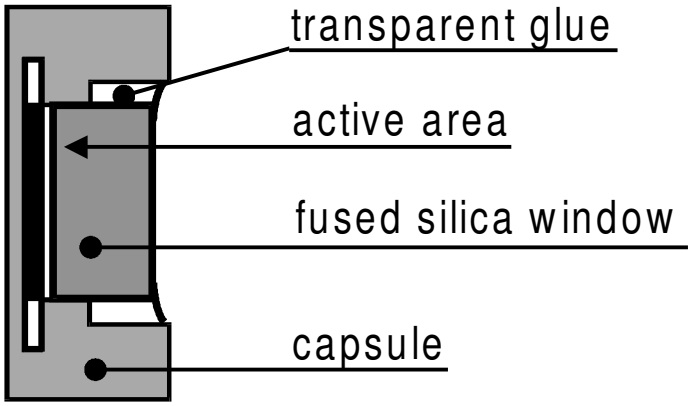

b) Hamamatsu APD

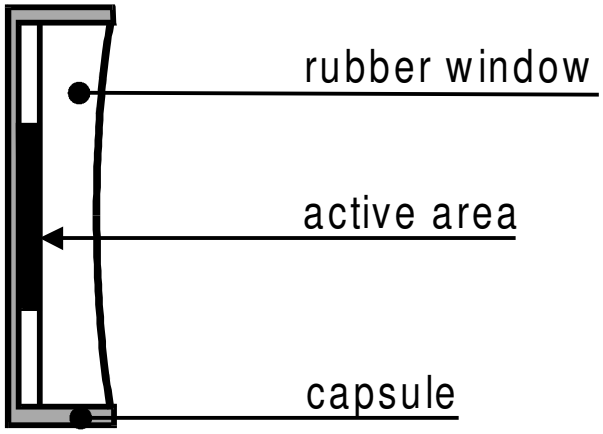

Fig. 1: section of APD's produced by EG&G and Hamamatsu. In both devices the Si wafer is enclosed in a capsule and covered with a transparent window. In the EG&G APD (Fig. 1a) the window is sealed to the capsule with some transparent glue. The Hamamatsu (Fig.1b) adopts a rubber window which completely fills the capsule-room and cover the Si surface together with the electric contacts (not reported in the figure).

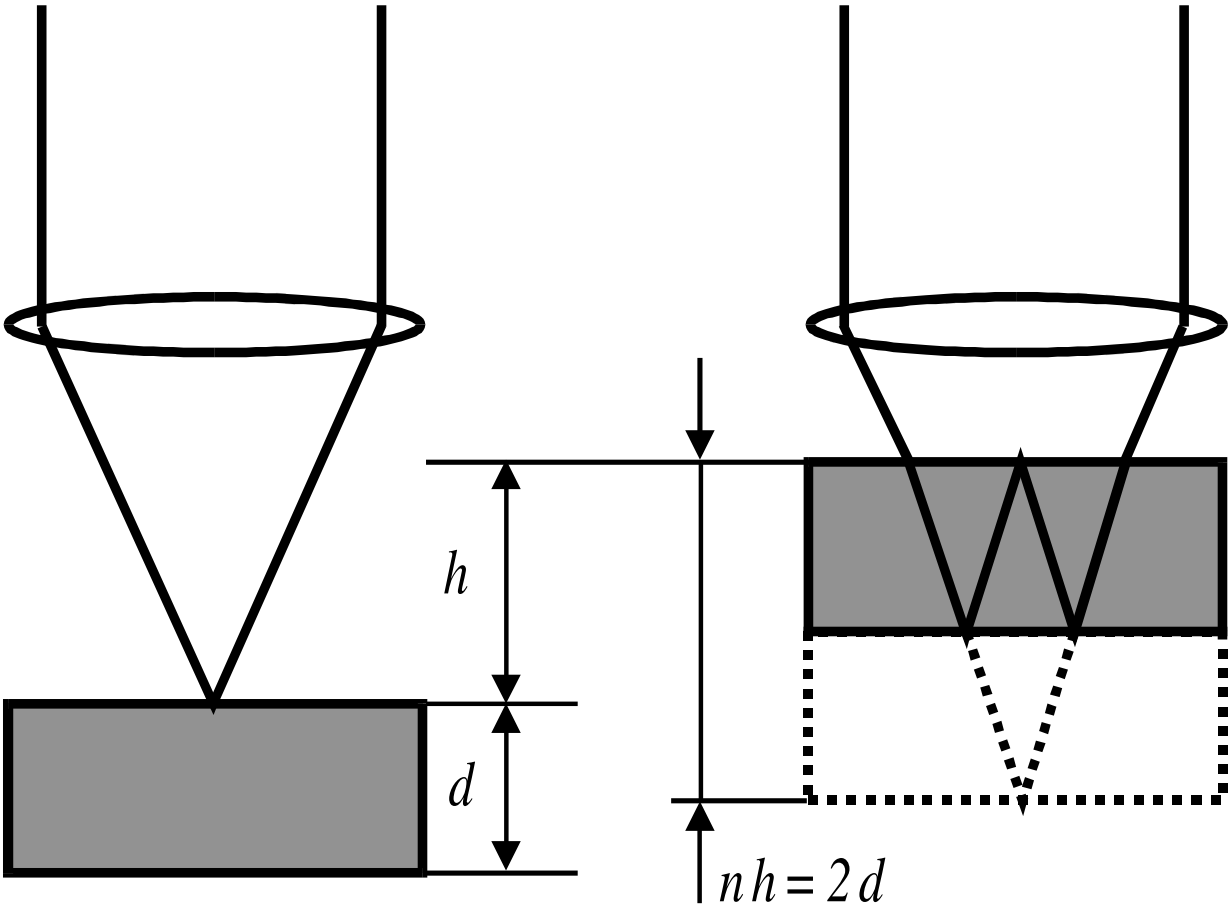

Fig. 2: determination of the window thickness (d) by an optical microscope: the difference between the heights of the microscope plate (h) for which, respectively, the window external surface and its image (reflected by the Si surface) are focused, correspond to the optical path $nh = 2d$, where n is the refractive index of the window.

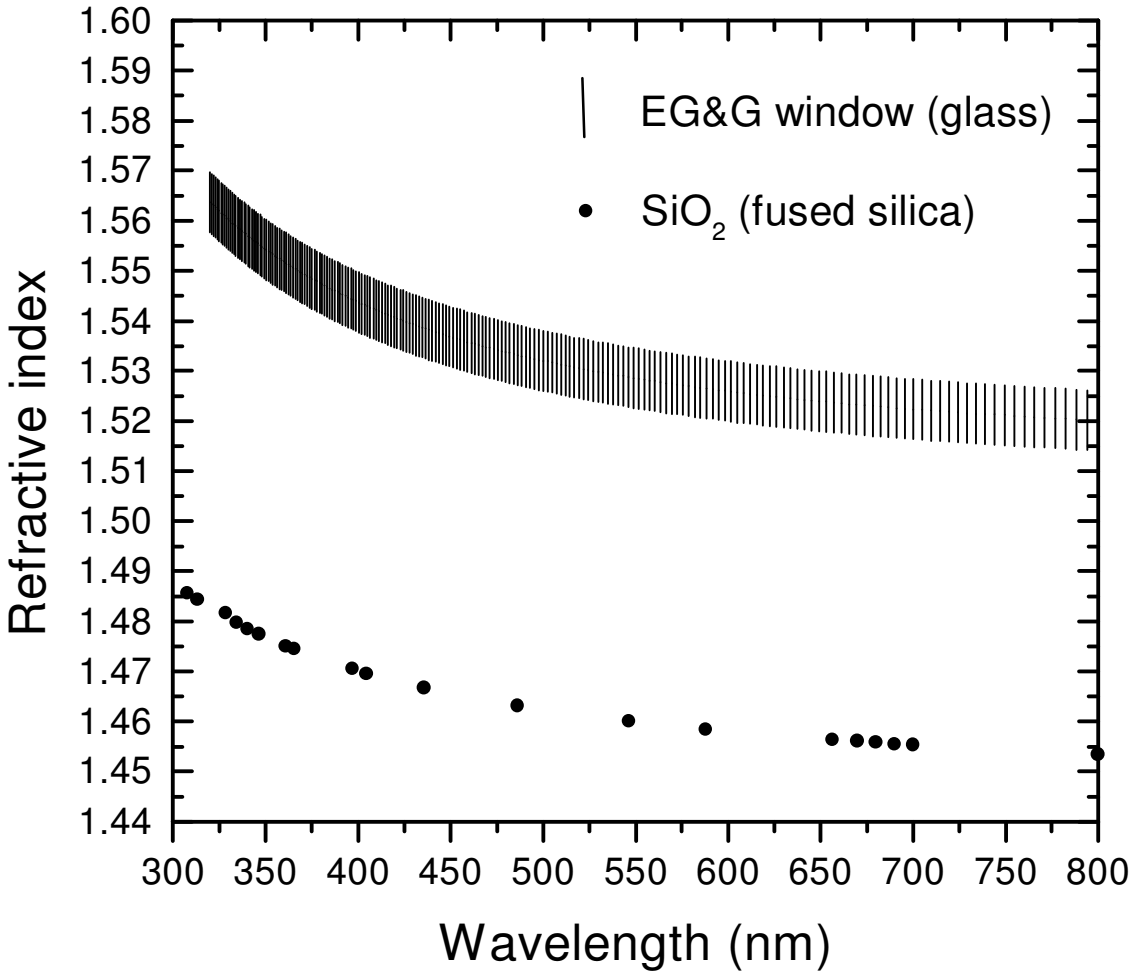

Fig. 3: experimentally determined refractive index of the EG&G APD window compared with the one of the SiO_2 (fused silica) [5] which, as discussed in the text, is assigned to the EG&G transparent glue (TG). In the same wavelength range, the extinction coefficient of the glass window is $k < 1\ 10^{-6}$.

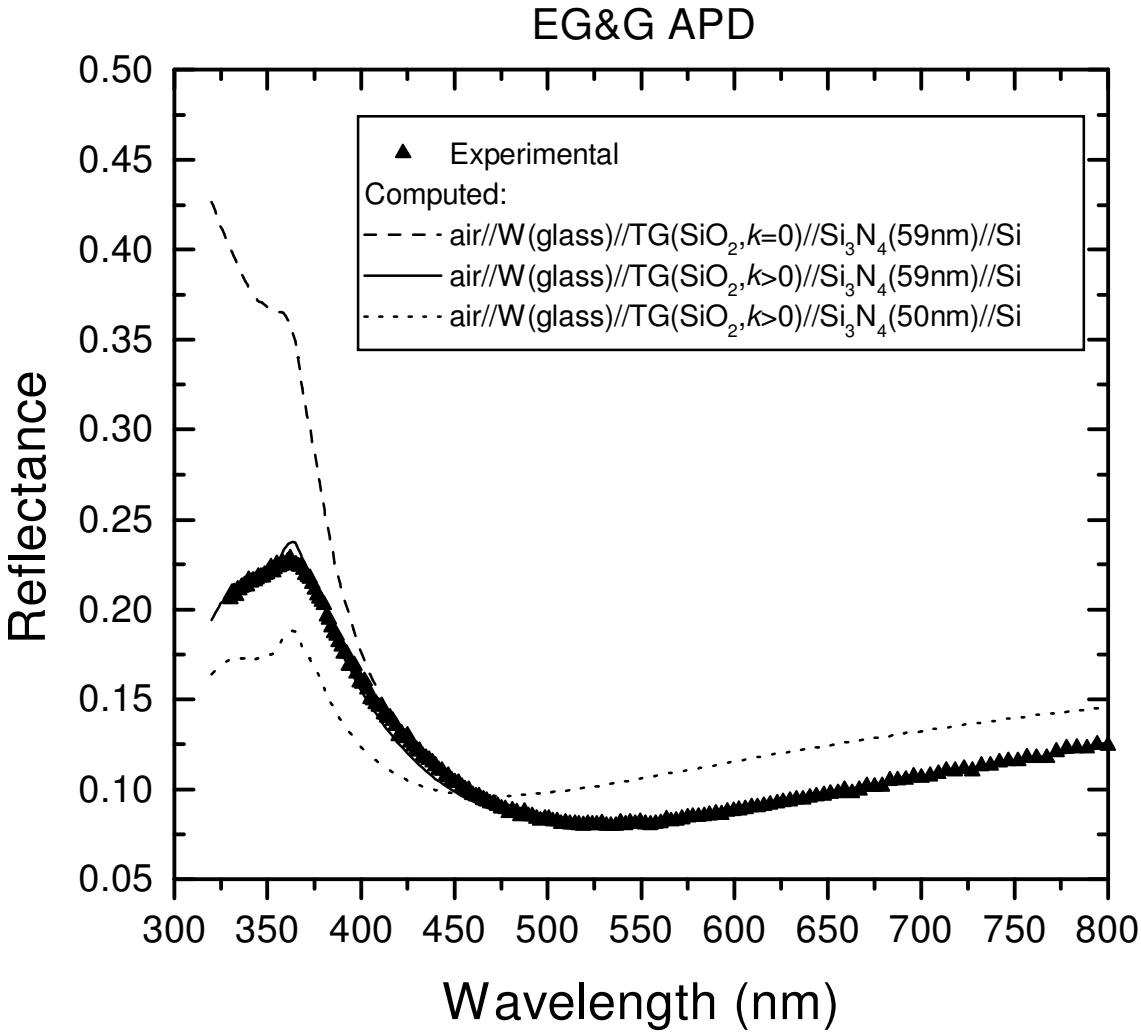

Fig. 4: reflectance of the "397A" EG&G APD compared with computed reflectances of several systems. A good agreement with the experimental data is obtained by considering the glass window sealed to the Si surface, coated with a 59nm thick Si_3N_4 film, with a transparent glue having the refractive index of SiO_2 (fused silica) and $k(\lambda)>0$ (see text). The effect of the Si_3N_4 antireflection coating is more effective in the 400-520 nm range when the coating thickness is about 50 nm.

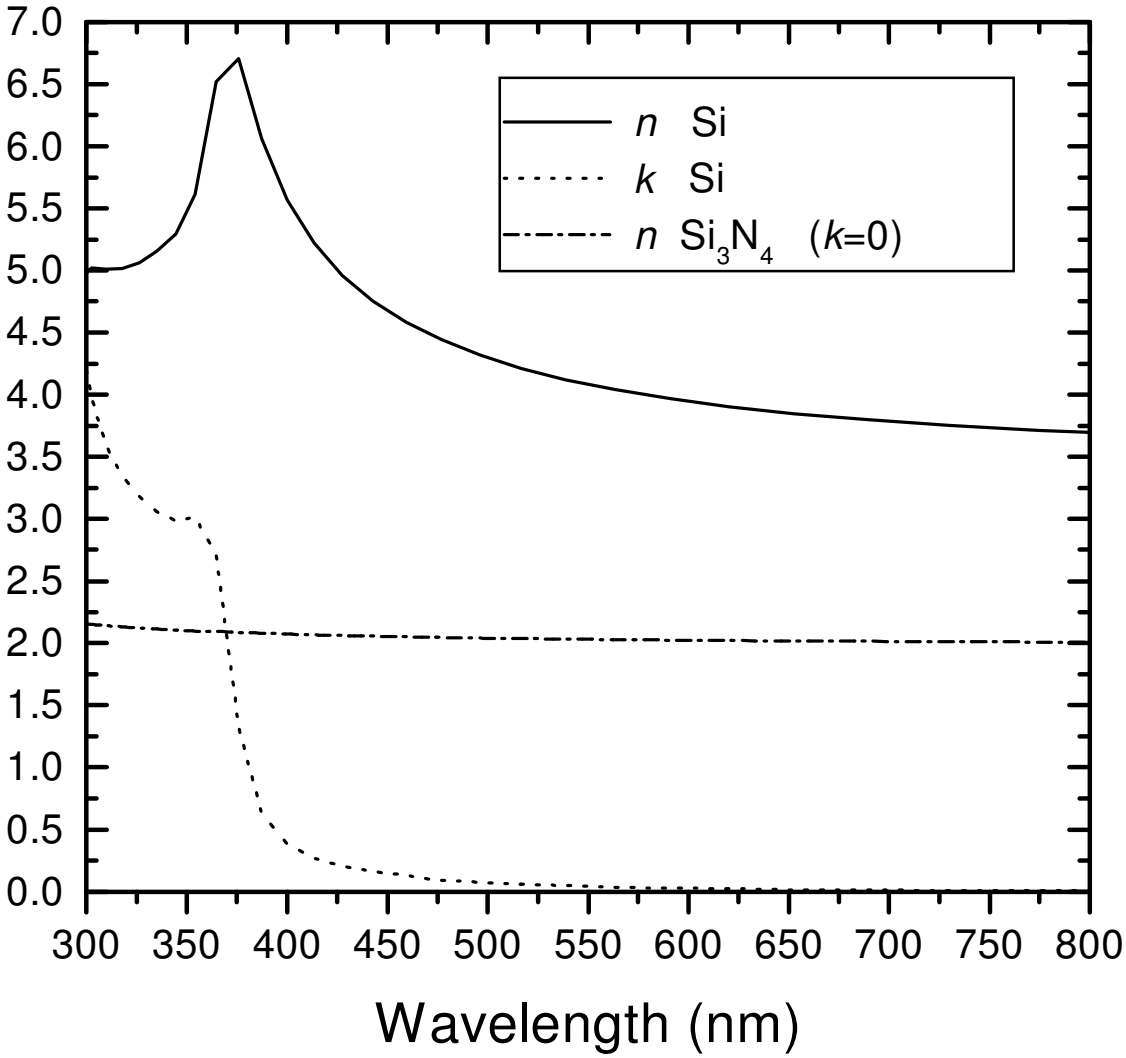

Fig. 5a: complex refractive indexes of Si and Si_3N_4 [5].

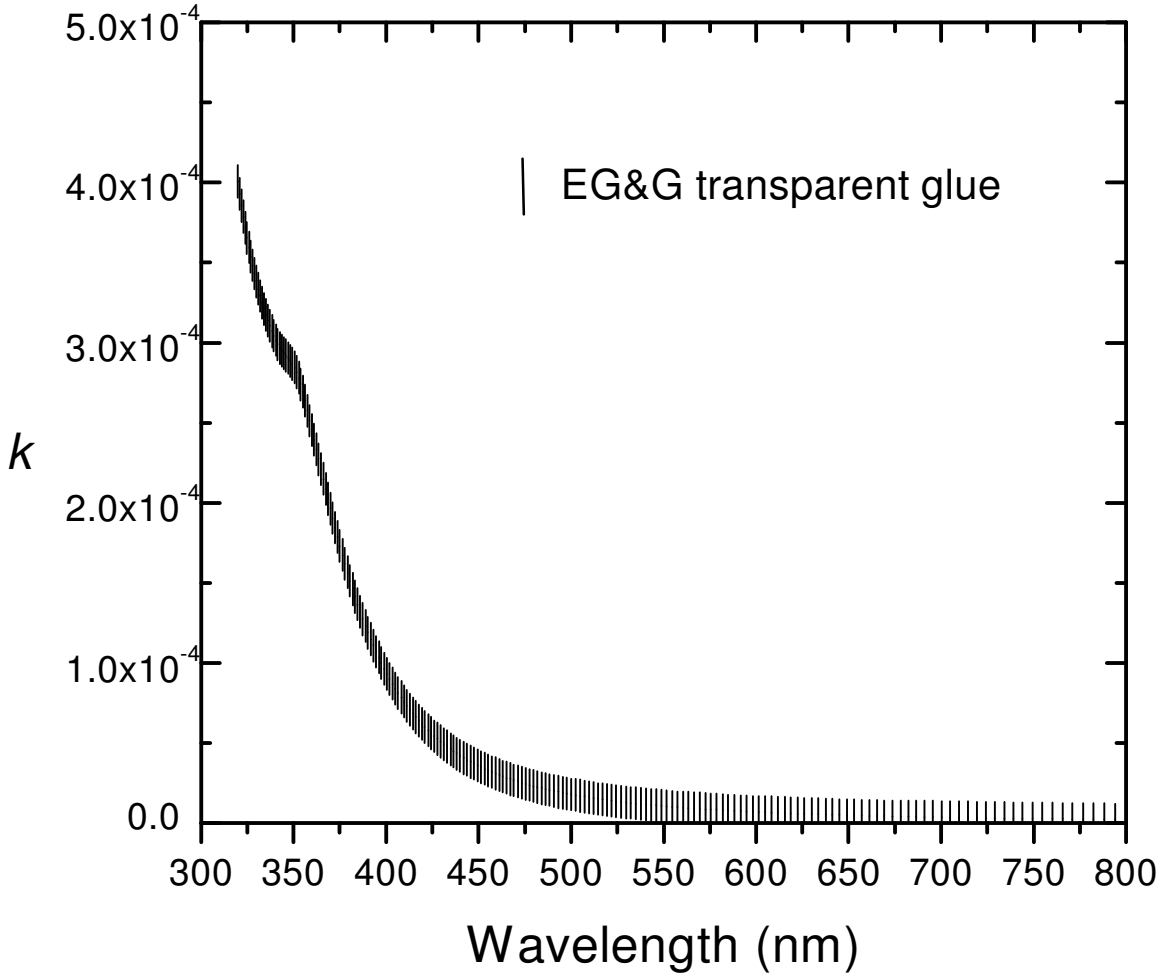

Fig 5b: extinction coefficient of the 30μm thick transparent glue (TG) layer, placed between window and Si in the EG&G APD, giving a good reproduction of the experimental reflectance measurement.

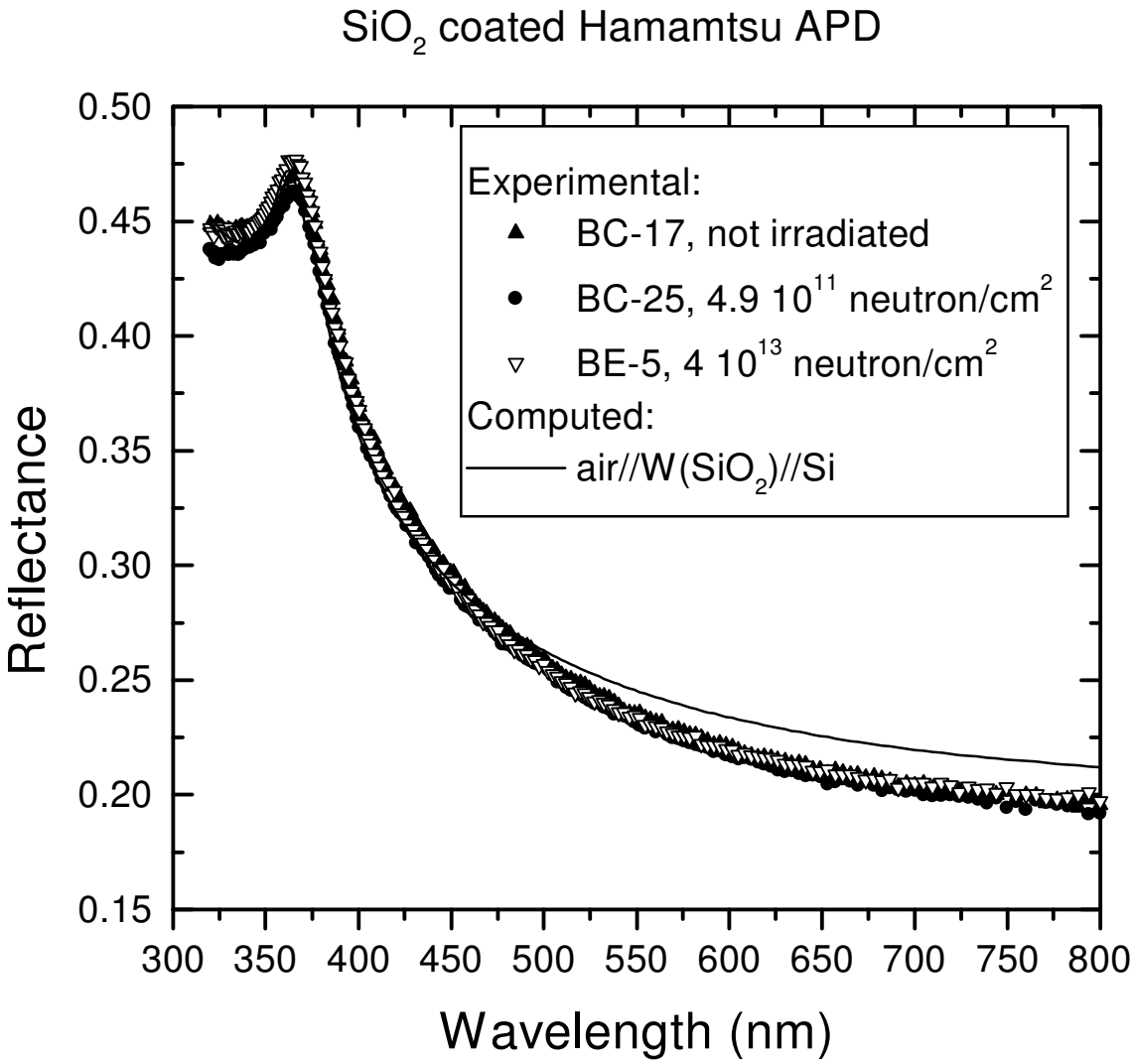

Fig. 6: reflectance of BC-17, BC-25 and BE-5 Hamamatsu APD, irradiated with neutrons at several doses compared with the reflectance computed according to the model "air//W//Si", where the refractive index of the rubber window (W) is assumed to be the same of the SiO_2 coating.

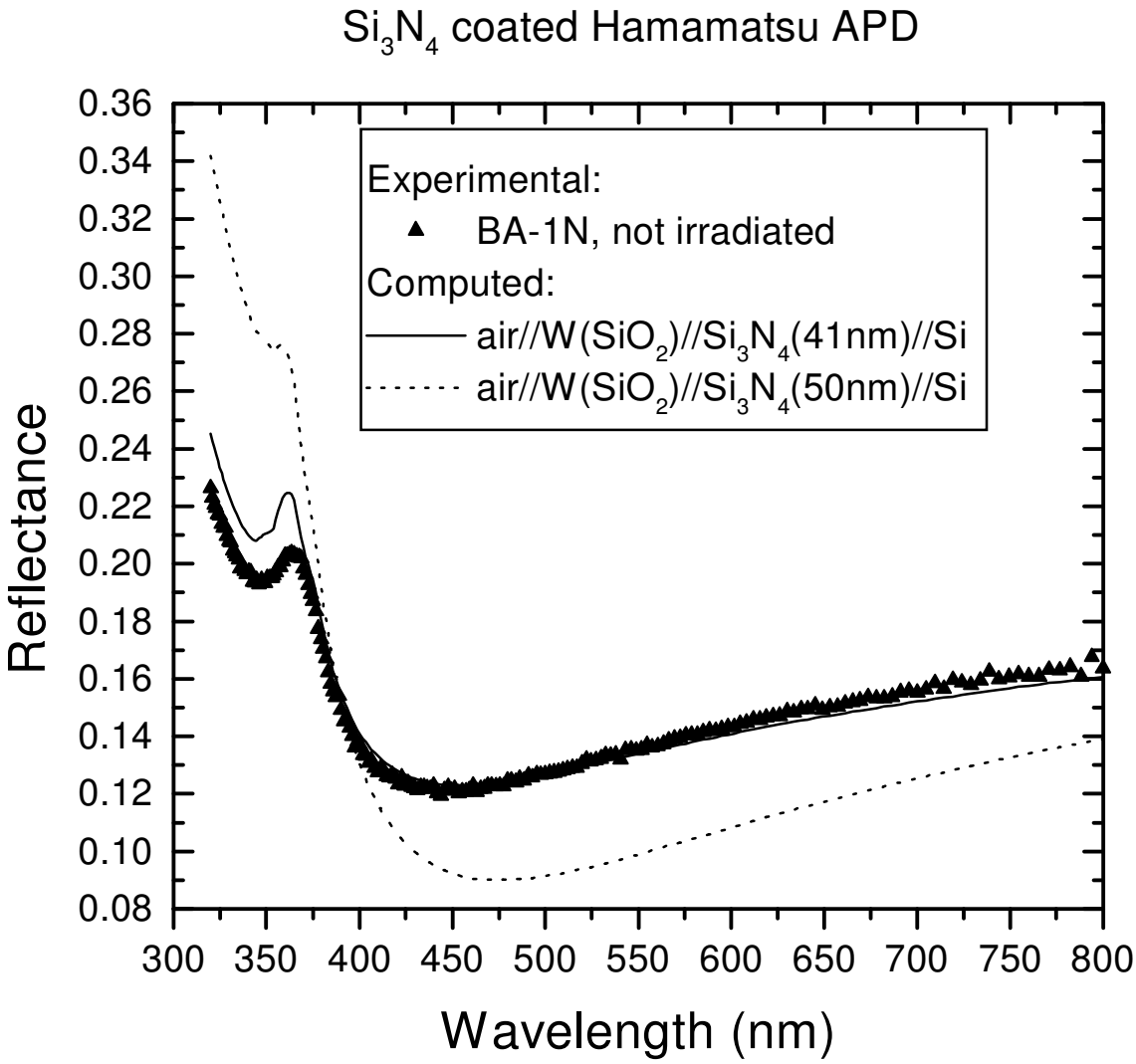

Fig. 7: reflectance of the Si_3N_4 coated "BA1N" Hamamatsu APD compared with the computed reflectance based on the model "air//W(SiO_2)//Si_3N_4(41nm)//Si". The effect of the Si_3N_4 antireflection coating is more effective in the 400-520 nm range when the coating thickness is about 50 nm.

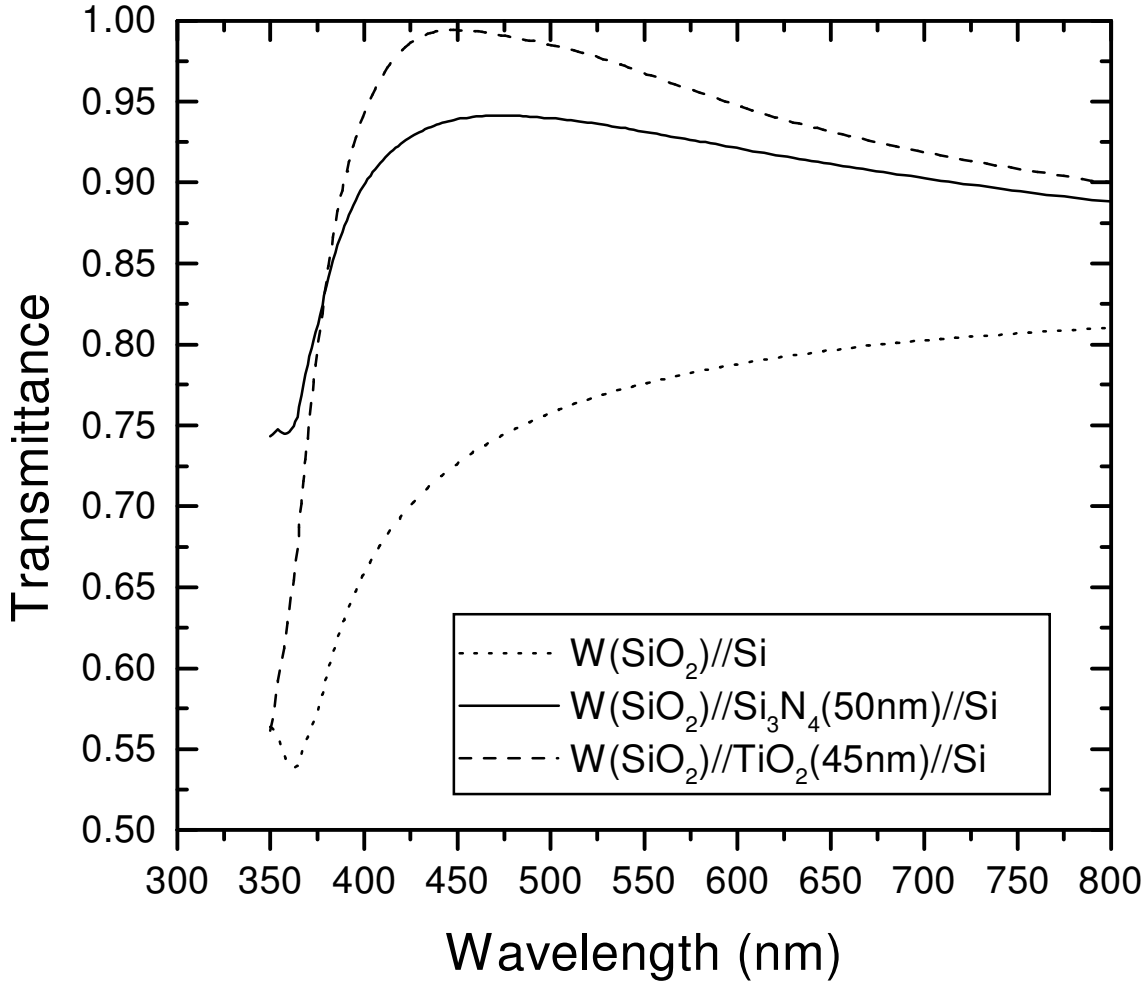

Fig. 8a: transmittance from $W(SiO_2)$ to the Si without and with Si_3N_4 (50nm) and TiO_2 (45nm) AR.

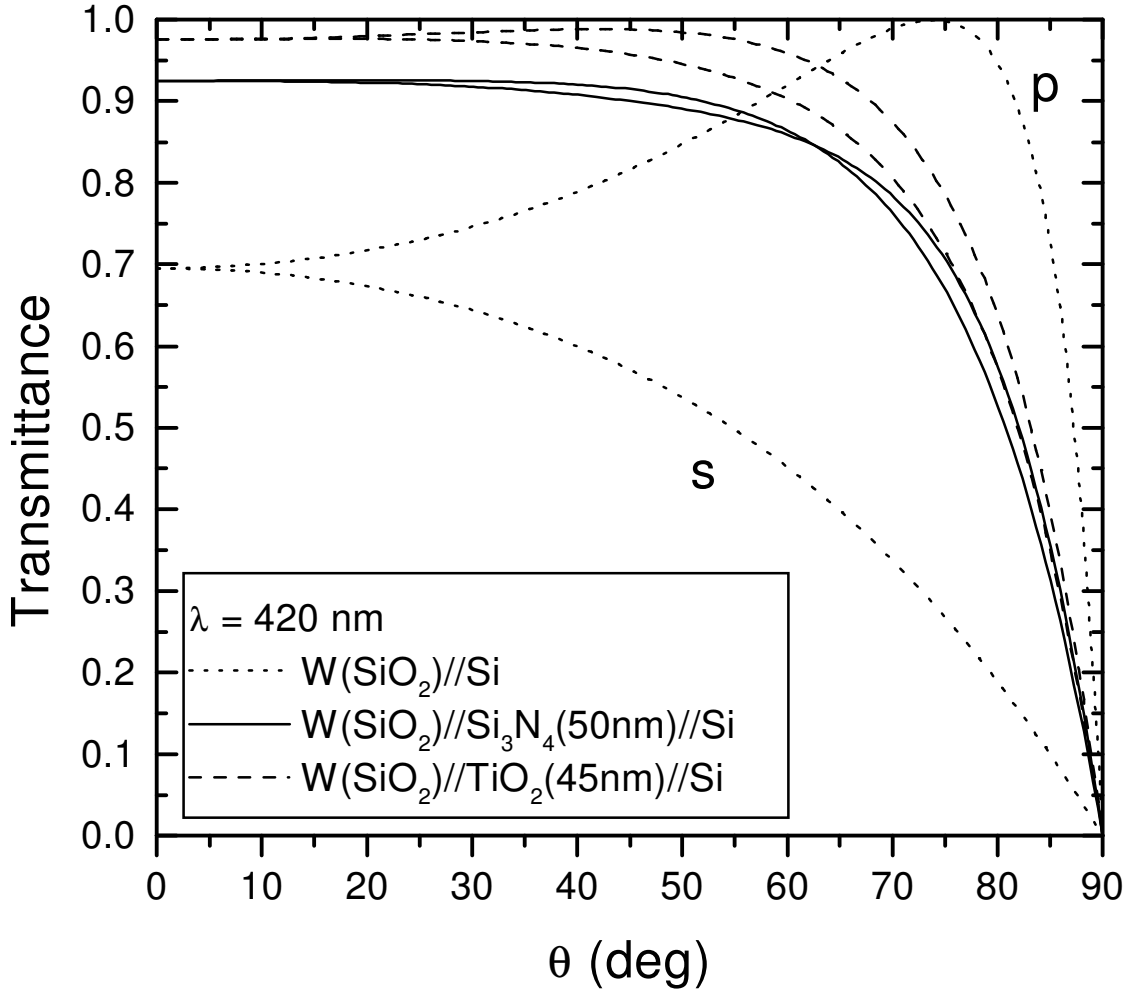

Fig. 8b: transmittance at 420 nm versus the incidence angle from $W(SiO_2)$ to the Si without and with Si_3N_4 (50nm) and TiO_2 (45nm) AR.

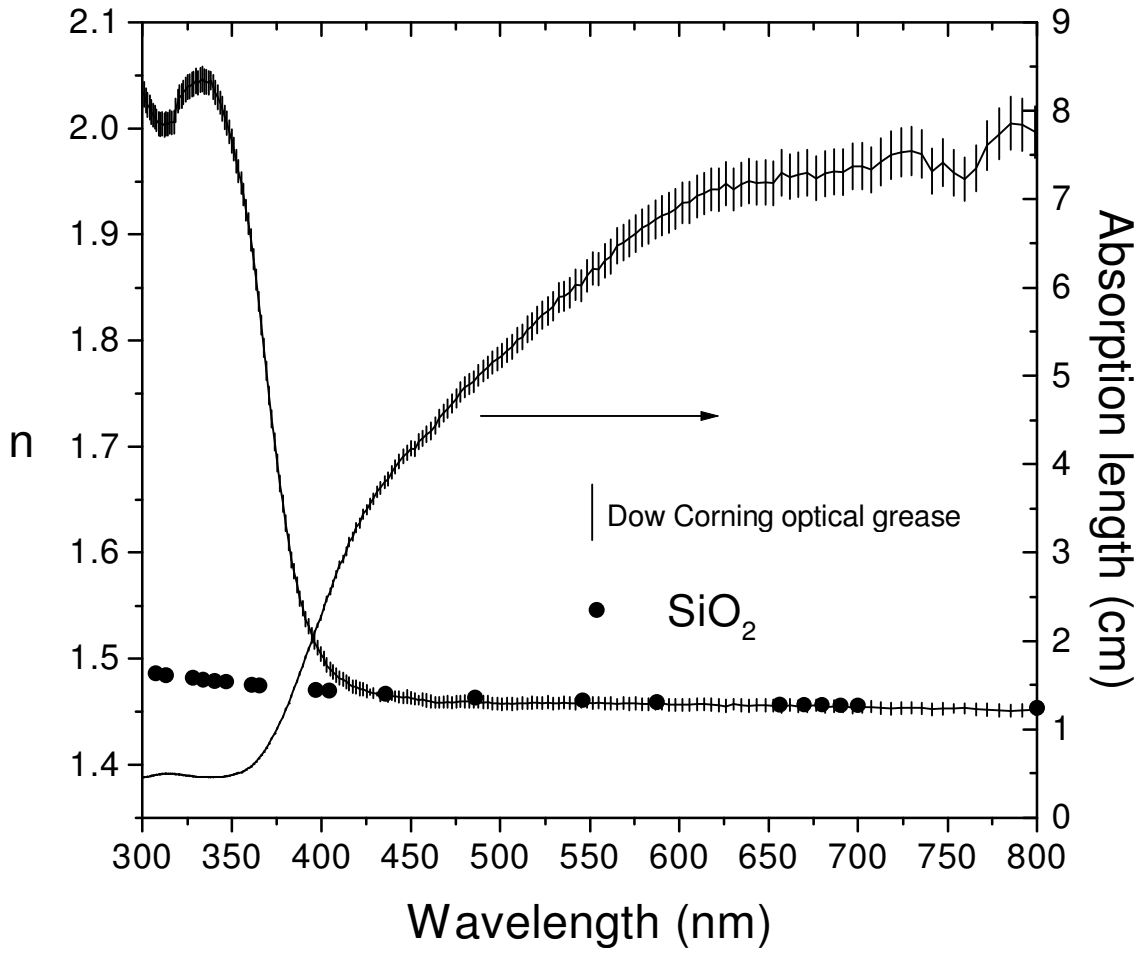

Fig. 9: measured refractive index and absorption length of the Dow Corning 02-3067 optical grease. For wavelengths greater than 400nm the refractive index is very similar to the SiO_2 (fused silica) one, also reported in figure [5].

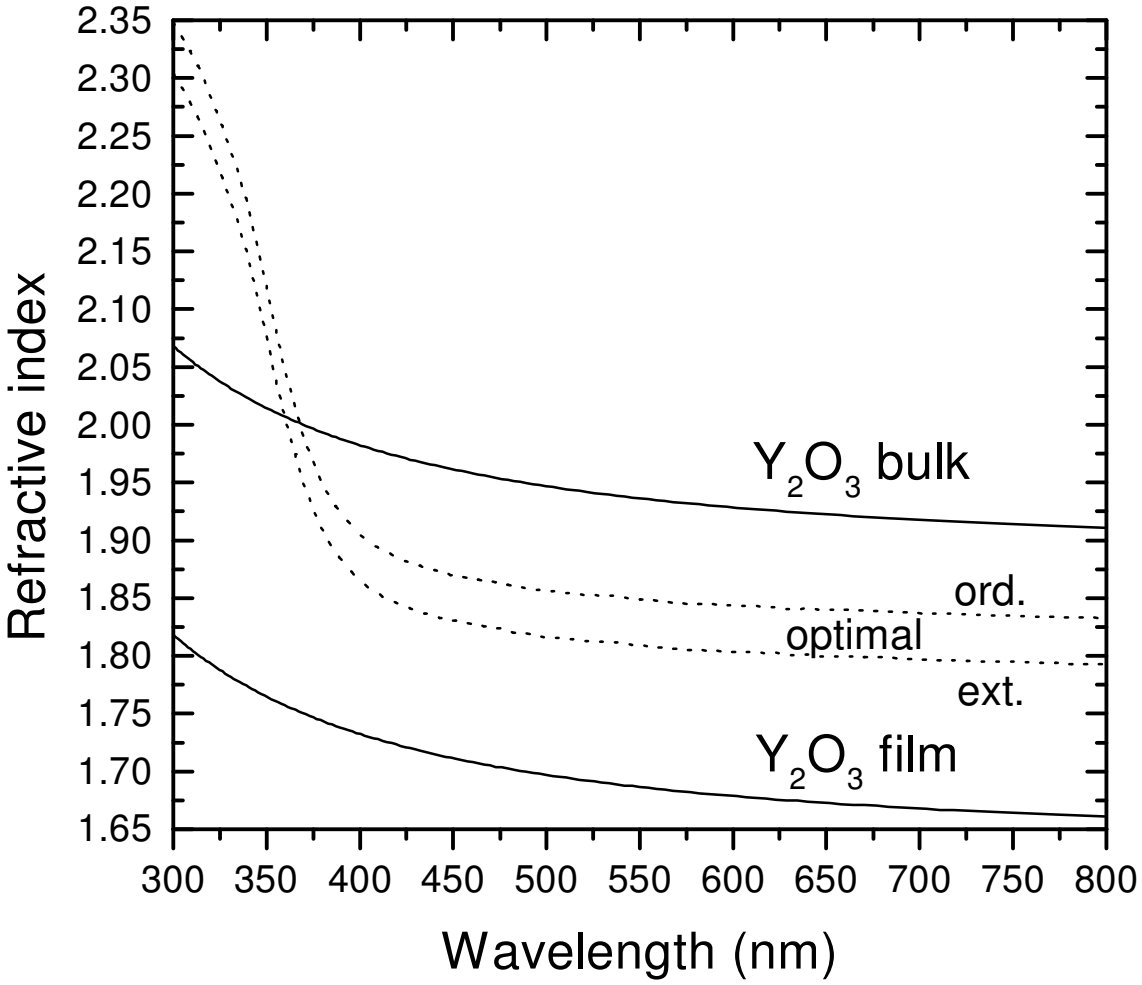

Fig. 10: refractive indexes of: a) the optimal AR coating for the PWO//DG interface ($\sqrt{n_{PWO} n_{DG}}$), both for the ordinary and the extraordinary PWO refractive indexes; b) Y_2O_3 bulk [7]; c) Y_2O_3 film deposited on the PWO test piece as computed from the measurements reported in Fig. 11.

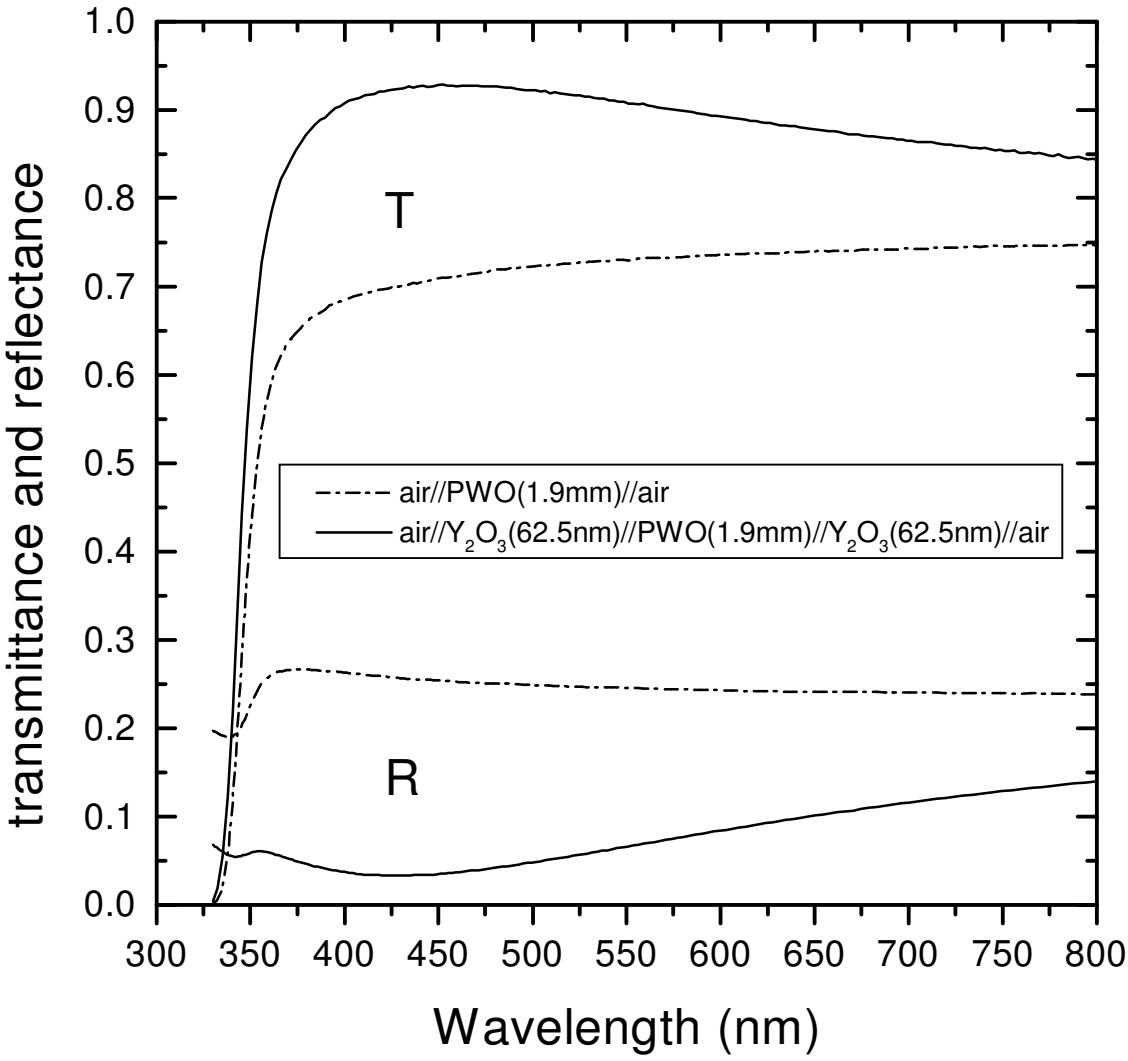

Fig. 11: transmittance and reflectance, at normal incidence, of the uncoated and coated PWO test piece. The experimental curves are well reproduced by assuming the films perfectly transparent (k=0), 62.5 nm thick and with the refractive index of a material composed by 76% in volume of Y_2O_3 [7] and 24% of air, computed according to the effective medium approximation [9].

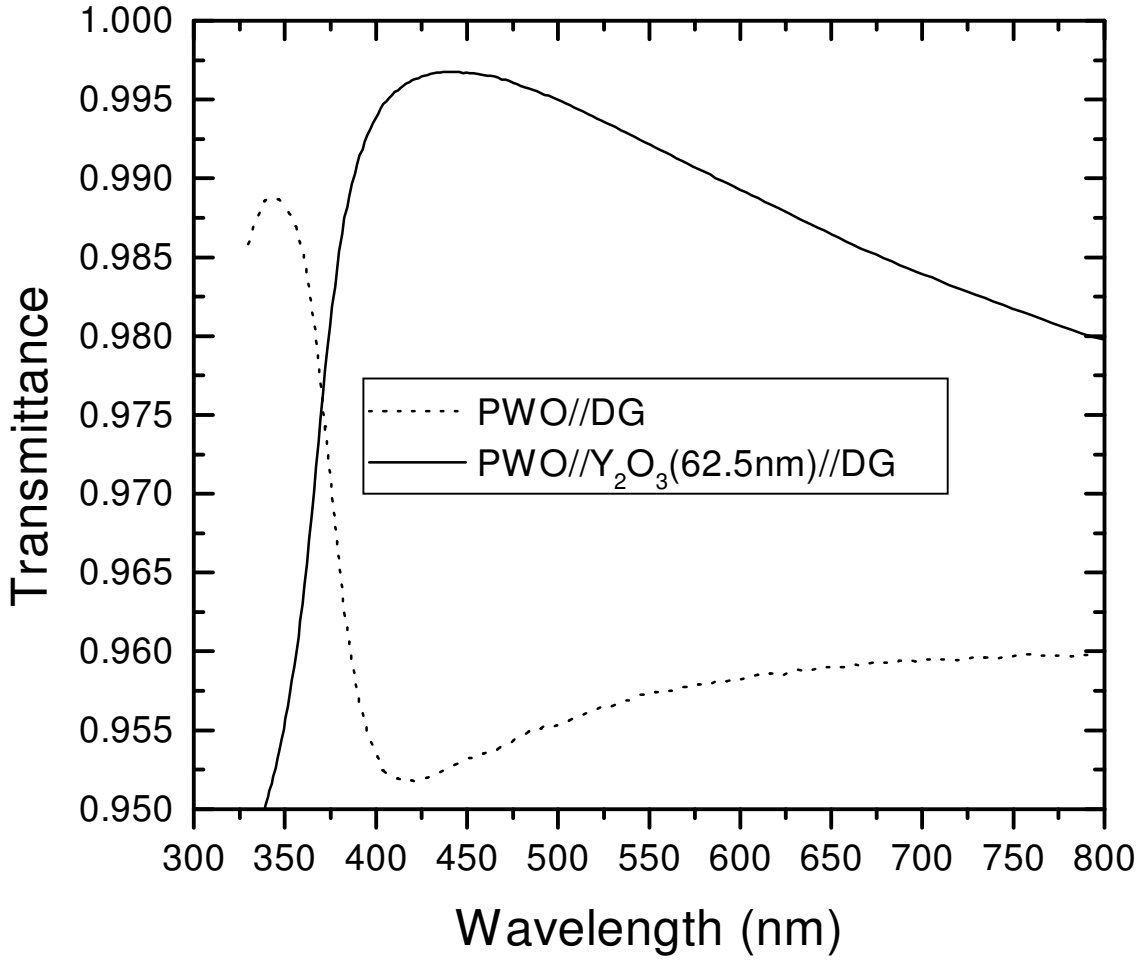

Fig. 12: simulated transmittance, at normal incidence, of the interfaces PWO//DG and PWO//Y_2O_3(62.5nm)//DG. With the AR coating the transmittance is about 4% greater than the uncoated case.

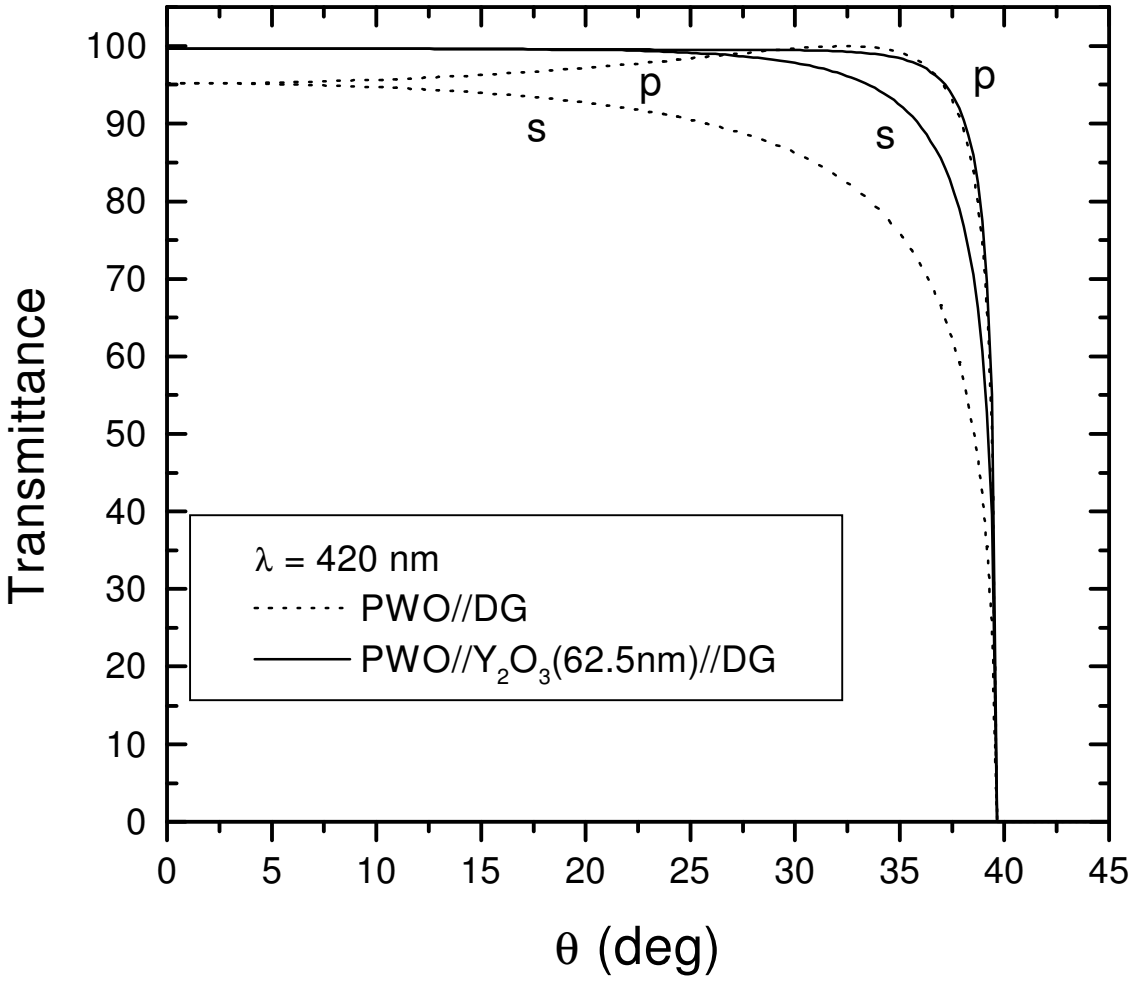

Fig. 13a: simulated transmittance versus the incidence angle at 420nm of the interfaces PWO//DG and PWO//Y_2O_3(62.5nm)//DG.

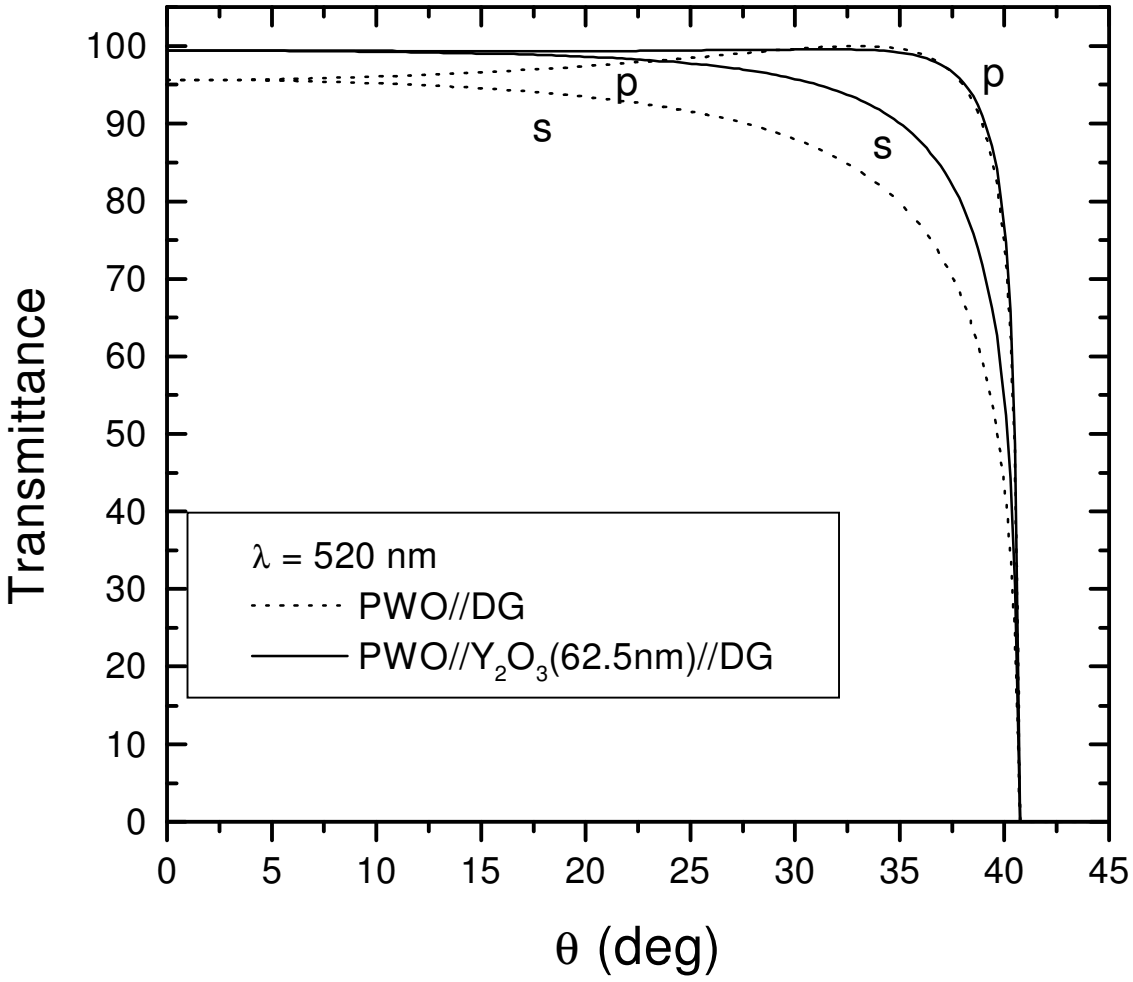

Fig. 13b: simulated transmittance versus incidence angle at 520nm of the interfaces PWO//DG and PWO//Y_2O_3(62.5nm)//DG.

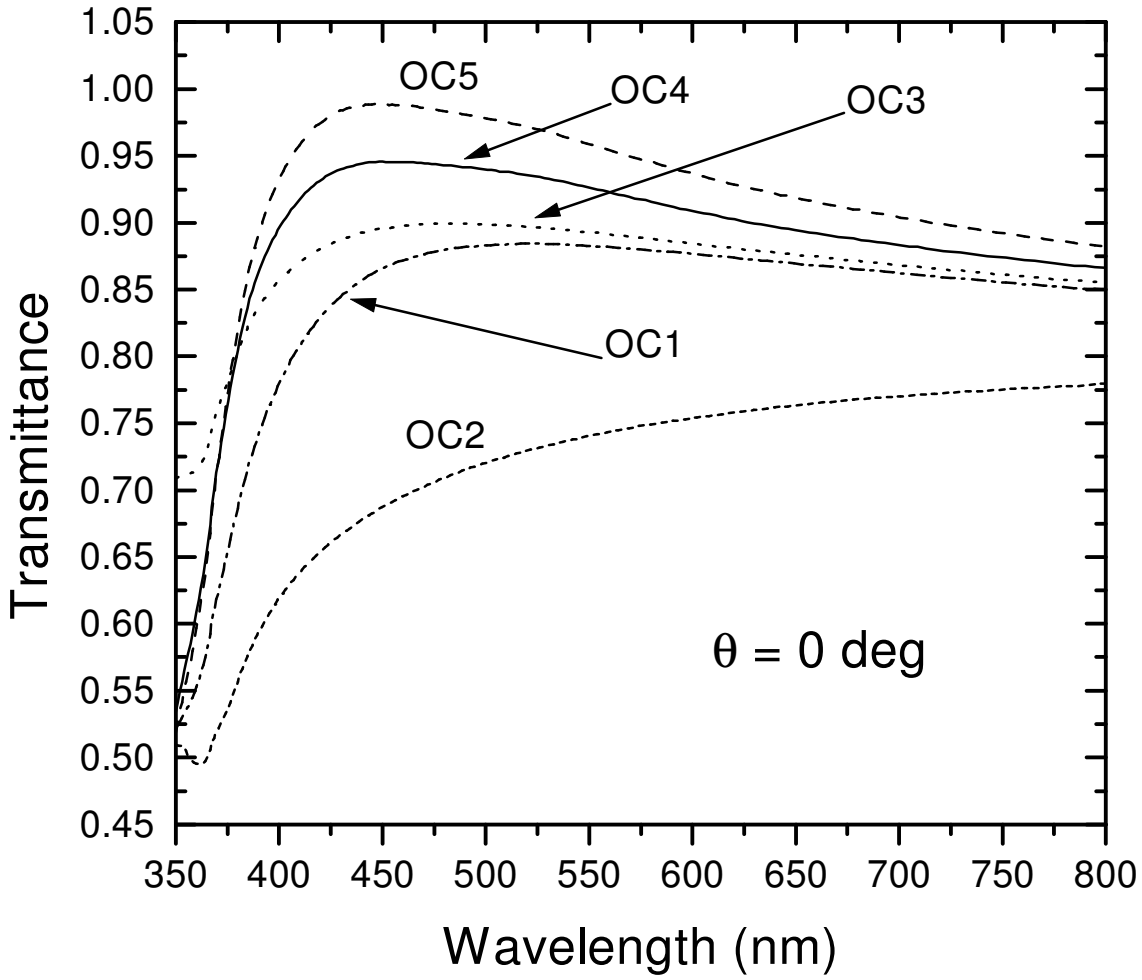

Fig. 14a: computed transmittance, from the PWO to the Si, at normal incidence for:
OC1: PWO//DG//W(glass)//TG(SiO_2,k>0)//Si_3N_4(50nm)//Si (EG&G APD) (line-dot);
OC2: PWO//DG//W(SiO_2)//SiO_2//Si (SiO_2 coated Hamamatsu APD) (short dash);
OC3: PWO//DG//W(SiO_2)//Si_3N_4(50nm)//Si (Si_3N_4 coated Hamamatsu APD) (dot);
OC4: PWO//DG//W(SiO_2)//TiO_2(45nm)//Si (line);
OC5: PWO//Y_2O_3(62.5nm)//DG//W(SiO_2)//TiO_2(45nm)//Si (dash).

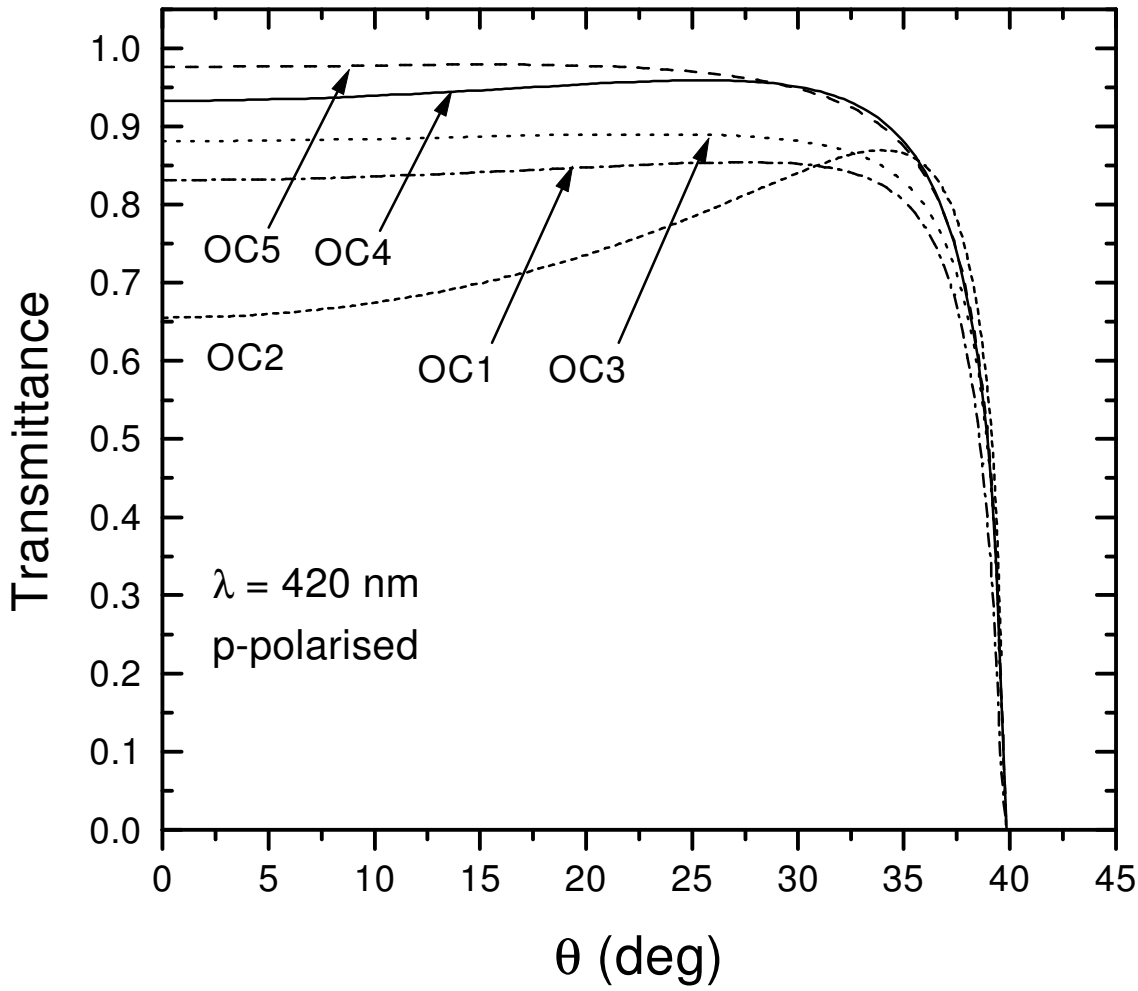

Fig. 14b: computed *p*-polarised transmittance, from the PWO to the Si, versus the incidence angle at 420nm for:

OC1: PWO//DG//W(glass)//TG(SiO_2,k>0)//Si_3N_4(50nm)//Si (EG&G APD) (line-dot);
OC2: PWO//DG//W(SiO_2)//SiO_2//Si (SiO_2 coated Hamamatsu APD) (short dash);
OC3: PWO//DG//W(SiO_2)//Si_3N_4(50nm)//Si (Si_3N_4 coated Hamamatsu APD) (dot);
OC4: PWO//DG//W(SiO_2)//TiO_2(45nm)//Si (line);
OC5: PWO//Y_2O_3(62.5nm)//DG//W(SiO_2)//TiO_2(45nm)//Si (dash).

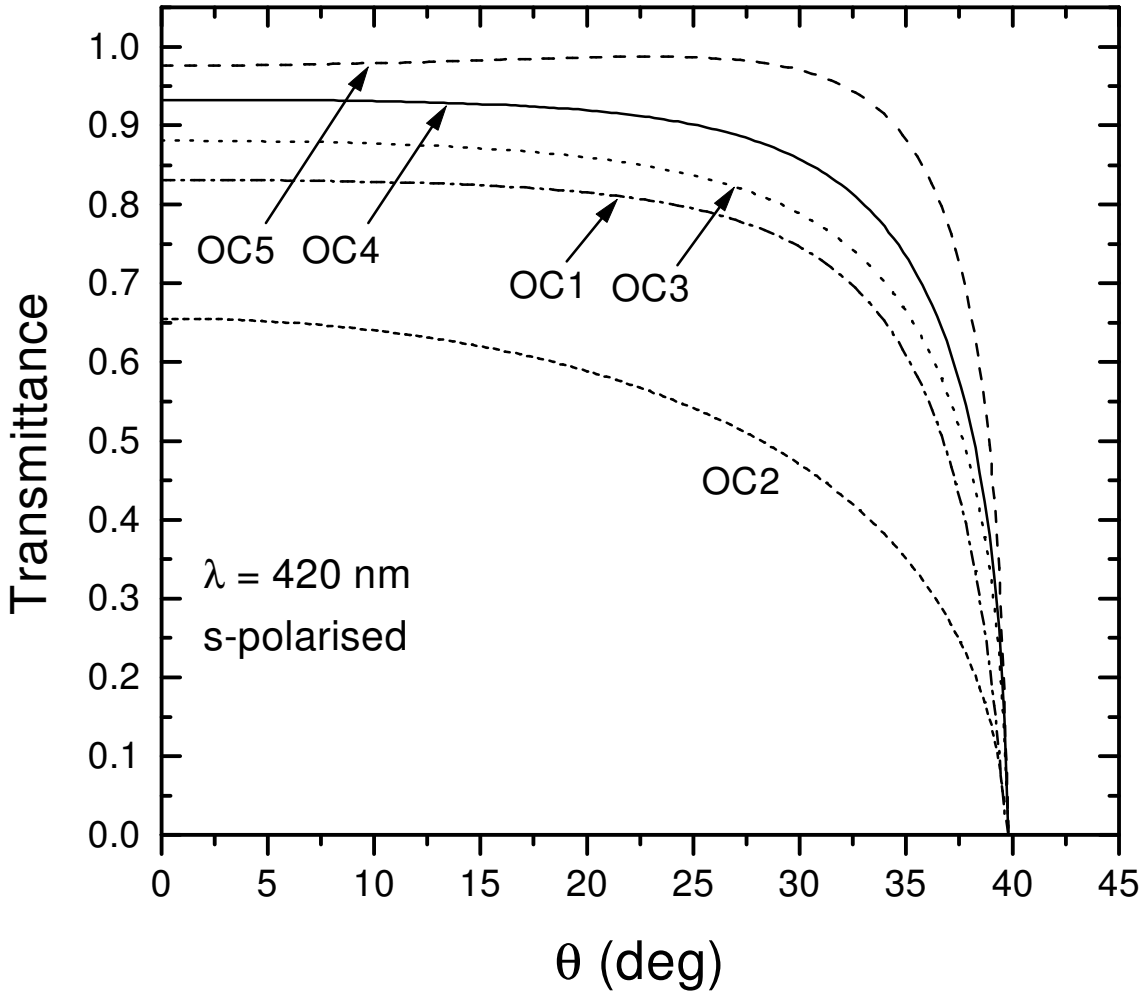

Fig. 14c: computed *s*-polarised transmittance, from the PWO to the Si, versus the incidence angle at 420nm for:

OC1: PWO//DG//W(glass)//TG(SiO_2,k>0)//Si_3N_4(50nm)//Si (EG&G APD) (line-dot);
OC2: PWO//DG//W(SiO_2)//SiO_2//Si (SiO_2 coated Hamamatsu APD) (short dash);
OC3: PWO//DG//W(SiO_2)//Si_3N_4(50nm)//Si (Si_3N_4 coated Hamamatsu APD) (dot);
OC4: PWO//DG//W(SiO_2)//TiO_2(45nm)//Si (line);
OC5: PWO//Y_2O_3(62.5nm)//DG//W(SiO_2)//TiO_2(45nm)//Si (dash).

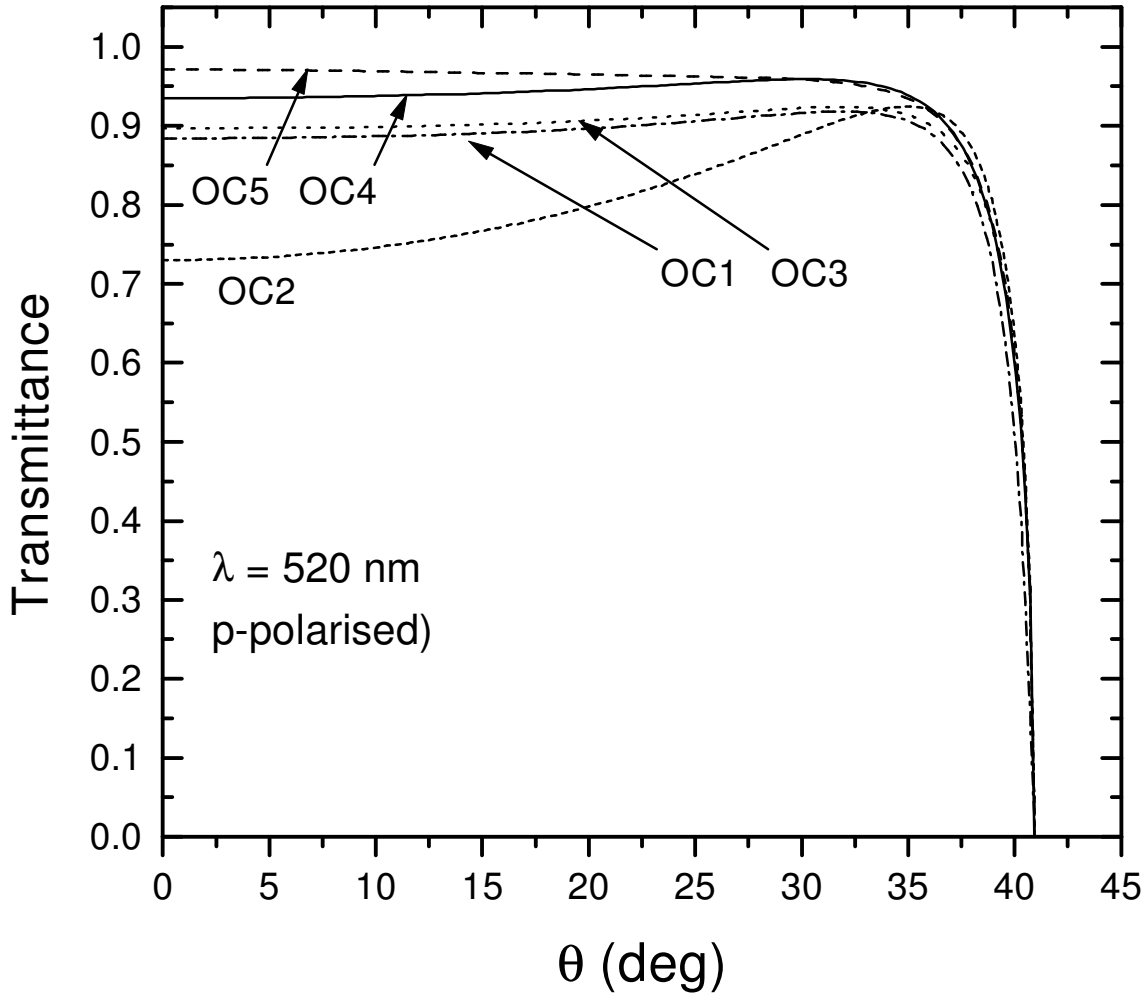

Fig. 14d: computed *p*-polarised transmittance, from the PWO to the Si, versus the incidence angle at 520nm for:

OC1: PWO//DG//W(glass)//TG(SiO_2,k>0)//Si_3N_4(50nm)//Si (EG&G APD) (line-dot);
OC2: PWO//DG//W(SiO_2)//SiO_2//Si (SiO_2 coated Hamamatsu APD) (short dash);
OC3: PWO//DG//W(SiO_2)//Si_3N_4(50nm)//Si (Si_3N_4 coated Hamamatsu APD) (dot);
OC4: PWO//DG//W(SiO_2)//TiO_2(45nm)//Si (line);
OC5: PWO//Y_2O_3(62.5nm)//DG//W(SiO_2)//TiO_2(45nm)//Si (dash).

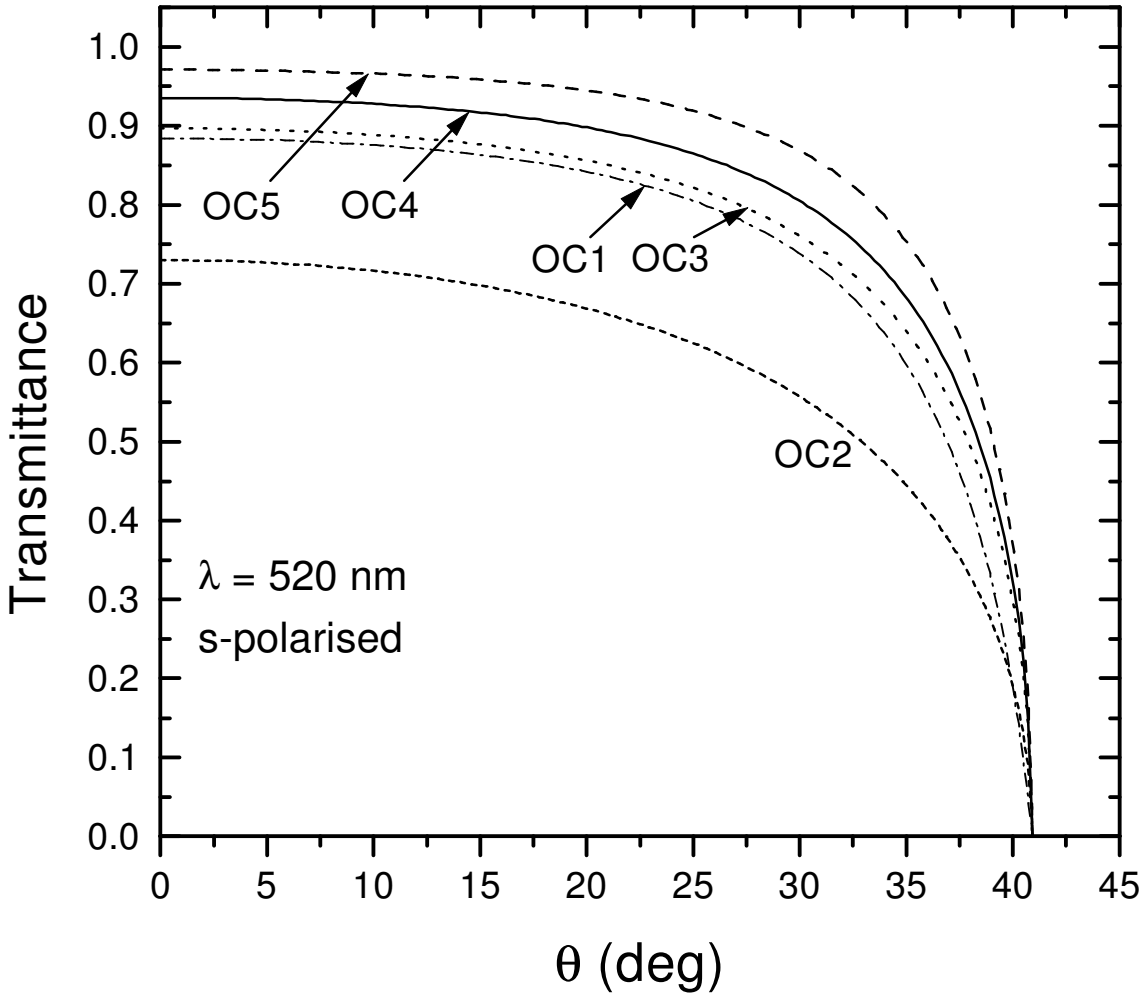

Fig. 14e: computed *s*-polarised transmittance, from the PWO to the Si, versus the incidence angle at 520nm for:

OC1: PWO//DG//W(glass)//TG(SiO_2,k>0)//Si_3N_4(50nm)//Si (EG&G APD) (line-dot);
OC2: PWO//DG//W(SiO_2)//SiO_2//Si (SiO_2 coated Hamamatsu APD) (short dash);
OC3: PWO//DG//W(SiO_2)//Si_3N_4(50nm)//Si (Si_3N_4 coated Hamamatsu APD) (dot);
OC4: PWO//DG//W(SiO_2)//TiO_2(45nm)//Si (line);
OC5: PWO//Y_2O_3(62.5nm)//DG//W(SiO_2)//TiO_2(45nm)//Si (dash).